MOL PHARM

MOLECULAR PHARMACOLOGY

Nuclear Translocation of Nuclear Transcription Factor-κB by α-Amino-3-hydroxy-5-methyl-4-isoxazolepropionic Acid Receptors Leads to Transcription of p53 and Cell Death in Dopaminergic Neurons

GABRIEL A. DE ERAUSQUIN, KRZYZTOF HYRC, DAVID A. DORSEY, DANIEL MAMAH, MEHMET DOKUCU, DANIEL H. MASCÓ, TIMOTHY WALTON, KRIKOR DIKRANIAN, MARIO SORIANO, JOSÉ MANUEL GARCÍA VERDUGO, MARK P. GOLDBERG, and LAURA L. DUGAN

Departments of Psychiatry (G.A.d.E., D.A.D., D.M., M.D., K.D.) and Neurology (G.A.d.E., T.W., M.P.G., L.L.D.) and Center for the Study of Nervous System Injury (G.A.d.E., K.H., M.P.G., L.L.D.), Washington University School of Medicine, St. Louis, Missouri; Departamento de Farmacología, Facultad de Ciencias Químicas, Universidad Nacional de Córdoba, Córdoba, Argentina (D.H.M.); and Departamento de Biología Celular, Universidad de Valencia, Valencia, Spain (M.S., J.M.G.V.)

This article is available online at http://molpharm.aspetjournals.org

ABSTRACT

We describe a new molecular mechanism of cell death by excitotoxicity mediated through nuclear transcription factor κB (NFκB) in rat embryonic cultures of dopaminergic neurons. Treatment of mesencephalic cultures with α-amino-3-hydroxy-5-methyl-4-isoxazolepropionic acid (AMPA) resulted in a number of changes that occurred selectively in dopaminergic neurons, including persistent elevation in intracellular Ca^{2+} monitored with Fura-2, and a significant increase in intramitochondrial oxidation of dihydrorhodamine 123, probably associated with transient increase of mitochondrial permeability, cytochrome c release, nuclear translocation of NFκB, and transcriptional activation of the oncogene p53. Interruption of any of these steps by specific antagonists prevented neurite pruning and programmed cell death. In contrast, cell death was not prevented by caspase antagonists and only partly prevented by nitric-oxide synthase inhibitors. This signal transduction pathway might be a contributing mechanism in ongoing neuronal death in Parkinson disease.

Parkinson disease (PD) is among the most prevalent neurological disorders in the elderly, and loss of mesencephalic dopaminergic neurons (DNs) is considered the cause of the motor symptoms of the illness. The reasons for the selective susceptibility of DNs in PD are poorly understood. Experimental and pathological data implicate a susceptibility of DNs to oxidative stress triggered by endogenous or exogenous toxins. Oxidative stress has been demonstrated in brain and in cell models of PD (Cassarino et al., 2000). In late stages of PD, the substantia nigra exhibits increased lipid peroxidation, superoxide dismutase activity, and iron content, and glutathione levels are decreased, very likely favoring oxidative stress (Hirsch et al., 1991; Jellinger et al., 1993). DNs may display an increased susceptibility to premature death because of poor calcium (Ca^{2+}) homeostasis (de Erausquin et al., 1994), insufficient Ca^{2+} buffering by Ca^{2+} binding proteins (German et al., 1992; Damier et al., 1999), increased requirement for trophic factor support, and abnormal proteosome degradation (McNaught and Jenner, 2001). In late PD stages, there is evidence of apoptosis (Mochizuki et al., 1996; Anglade et al., 1997), but other forms of cell death may also play a role (Jellinger, 2001). Direct damage to macromolecules by lipid peroxidation (Jenner, 1998) or release of tumor necrosis factor α (TNFα) by microglia (Hunot et al., 1997; Hartmann et al., 2002) has been suggested. Transcription factor NFκB nuclear translocation—which

aspet

ABBREVIATIONS: PD, Parkinson disease; DN, dopaminergic neuron; TNF, tumor necrosis factor; NFκB, nuclear transcription factor κB; GluR, glutamate receptor; AMPA, α-amino-3-hydroxy-5-methyl-4-isoxazolepropionic acid; ROS, reactive oxygen species; TH, tyrosine hydroxylase; phos-p53, phosphoprotein p53; MAP2, microtubule associated protein 2; EM, electron microscopy; 5,7-DHT, 5,7-dihydroxitryptamine; DHR123, dihydrorhodamine 123; DTT, dithiothreitol; PMSF, phenylmethylsulfonyl fluoride; EMSA, electrophoretic mobility shift assay; ELISA, enzyme-linked immunosorbent assay; PCR, polymerase chain reaction; NBQX, 1,2,3,4-tetrahydro-6-nitro-2,3-dioxo-benzo[f]quinoxaline-7-sulfonamide; NAS, 1-napthyl-acetyl spermine trihydrochloride; CSA, cyclosporin A; DEA/NO, sodium 1-(N,N-diethylamino)diazen-1-ium-1,2-diolate; PDTC, pyrrolidine dithiocarbamate; LTCC, L-type Ca^{2+} channel; Cyt-c, cytochrome c; mPT, mitochondrial permeability transition; NO, nitric oxide NOS, nitric-oxide synthase.

may be triggered by TNFα—is found during post-mortem examination to be increased in brains of persons with PD (Hunot et al., 1997). The relevance of this mechanism in PD was questioned (Jellinger, 2001), in part because NFκB is neuroprotective in other neuronal phenotypes (Mattson et al., 2000).

To elucidate the mechanism of susceptibility of DNs, we studied cultures of mesencephalon, which allow in vitro comparisons of individual DNs with neurons expressing other phenotypes. In this system, DNs show unique physiologic properties— compared with nondopaminergic neurons—and, like DNs in vivo (Bywood and Johnson, 2000), are selectively susceptible to GluR$_{AMPA}$ receptor agonists (de Erausquin et al., 1994; Isaacs et al., 1996). DN susceptibility to GluR$_{AMPA}$ agonist toxicity is phenotype-specific, because other neuronal phenotypes in vitro display trophic responses or physiologic effects, but not toxicity (de Erausquin et al., 1994; Isaacs et al., 1996). After treatment with (S)-α-amino-3-hydroxy-5-methyl-4-isoxazolepropionic acid (AMPA), DNs selectively display [Ca^{2+}]$_i$ accumulation, either because DNs lack adequate [Ca^{2+}]$_i$ buffering capacity (Isaacs et al., 1996), because they have larger functionally available [Ca^{2+}]$_i$ stores (de Erausquin et al., 1994), or both. We tested the hypothesis that AMPA-induced injury to DNs is mediated through activation of the reactive oxygen species (ROS)-sensitive transcription factor NFκB and the oncogene *p53*; we postulate that this signaling pathway could account for the increased NFκB translocation observed post-mortem in PD.

Materials and Methods

Experimental Procedures and Immunohistochemistry

Cultures. Cultures were prepared as described previously (de Erausquin et al., 1992). Briefly, ventral mesencephali from day 15 rat embryos (Sprague-Dawley timed mothers; Charles River Laboratories, Wilmington, MA) were mechanically dissociated and plated at a density of 30 to 50,000 cells/cm^2 on dishes or multiwell plates coated with 15 mg/ml poly(D-lysine) (M$_r$ 53,000; Sigma, St. Louis, MO) and 10 mg/ml laminin (Sigma). The culture medium contained Dulbecco's modified Eagle's medium/Ham's F12 medium (50%/50%) (Invitrogen, Carlsbad CA), 25 mM glucose, 2 mM glutamine, 10% horse serum (Hyclone, Logan, UT), bFGF (10 ng in 500 ml; Sigma), and insulin-transferrin-sodium selenite media supplement (Sigma). Cells were cultured 9 days at 37°C in an atmosphere of 95% air/5% CO$_2$ saturated with H$_2$O.

AMPA Toxicity. Culture medium was exchanged with conditioned medium containing 10, 30, or 100 μM AMPA alone or in combination with drugs (Isaacs et al., 1996). Cells were then returned to the incubator for the length of the experiment (24 h for viability). Drugs were dissolved in HEPES-buffered saline solution (116 mM NaCl, 5.4 mM KCl, 0.8 mM MgSO$_4$, 1.8 mM NaH$_2$PO$_4$, 12 mM HEPES, 25 mM NaHCO$_3$, and 5.5 mM D-glucose, pH 7.4).

Immunohistochemistry. Cultures were fixed in phosphate-buffered saline containing 4% paraformaldehyde and 0.5% glutaraldehyde for 30 min at room temperature; permeabilized in 0.25% Triton X-100 for 10 min; blocked in 10% goat serum; and incubated in primary antibody, followed by conjugated secondary antibody (Alexa-488 or Alexa-568; Molecular Probes, Eugene, OR). Monoclonal or polyclonal antibodies were from commercial sources: tyrosine hydroxylase (TH; Pelfreeze, Rogers, AK; or Chemicon, Temecula, CA), MAP2 (Roche Molecular Biochemicals, Indianapolis IN), synapsin-1 (Chemicon), IκBα (Abcam, Cambridge, UK), NFκBp65 (Santa Cruz Biotechnologies, Santa Cruz, CA), cytochrome *c* (BD Biosciences PharMingen, San Diego, CA), phosphoprotein p53 (phos-p53; Zymed, South San Francisco, CA).

Neuronal Survival. Cultures immunostained with microtubule associated protein 2 (MAP2) and TH were counted. The number of fields required to count 1000 cells on control wells (typically 52 fields at 200×) was matched in experimental wells. Values represent averages of at least three experiments.

Neurite Morphology. Digital images of DNs were captured with a cooled charge-coupled device camera (Nikon Diaphot, Nikon Apo 20× dry objective; Nikon, Tokyo, Japan), and analyzed (MetaMorph; Universal Imaging, WestChester, PA). Cell process number, length, and branch frequency were counted; lengths were measured in pixels, transformed to micrometers using standard rulers, and averaged for each cell.

Electron Microscopy. Cultures were fixed, stained with immunoperoxidase-diaminobenzidine, dehydrated, embedded in an epon/araldite mix, and cut for light (1.0 μm) or electron microscopy (EM) (80 nm). For EM (Philips EM300 TEM), sections were mounted on copper grids and stained with uranyl acetate and lead citrate. DNs were identifiable by the presence of the chromogen.

Identification of DNs. DNs were distinguished by uptake of 5,7-dihydroxitryptamine (5,7-DHT) by briefly viewing cultures under fluorescence (excitation, 360 nm; emission, 420 nm; Silva et al., 1988; de Erausquin et al., 1992); phase contrast was used to allow relocation. Rapid bleaching of 5,7-DHT prevented interference with further imaging.

DHR123 Fluorescence. Cultures incubated with dihydrorhodamine 123 (DHR123) were imaged using a laser scanning confocal microscope (Noran Odyssey equiped with an argon-ion laser; excitation, 488 nm; emission, 515 nm) coupled to an inverted microscope (Nikon Diaphot; 60× oil immersion objective Nikon Plan Apo) (Dugan et al., 1995). Frame-averaged images were analyzed using regions of interest (MetaMorph). All drugs were added in a small aliquot of buffer (50 μl).

NFκB Activation

Nuclear Extracts. Experiments were terminated with iced lysis buffer [10 mM KCl, 1.5 mM MgCl$_2$, 0.5 mM dithiothreitol (DTT), 0.5 mM phenylmethylsulfonyl fluoride (PMSF), and 10 mM HEPES, pH 7.9, plus 2 mg/ml pepstatin A, 2 mg/ml leupeptin, and 2 mg/ml L-leucinethiol]. Samples were homogenized, incubated on Nonidet P-40, and centrifuged. Pellets were resuspended in extraction buffer (420 mM NaCl, 1.5 mM MgCl$_2$, 0.2 mM EDTA, 0.5 mM DTT, 0.5 mM PMSF, and 20 mM HEPES, pH 7.9, plus 2 mg/ml pepstatin A, 2 mg/ml leupeptin, and 2 mg/ml L-leucinethiol) and centrifuged for 15 min at 12,500 rpm (4°C). The supernatant containing the nuclear extracts was saved, and protein concentration determined (Invitrogen).

Electrophoretic Mobility Shift Assay. EMSAs were performed using a commercially available kit (Boehringer Ingelheim, Petersburg, VA). Aliquots incubated 15 min with 1 × 10^5 cpm of ^{32}P–end-labeled, double-stranded oligonucleotide (5′-TCAGAGGGGACTTTC-CGAGAGG-3′) were run on 6% polyacrylamide gels for 105 min with 150 V (reaction buffer, 500 mM NaCl, 5 mM EDTA, 5 mM DTT, 50 mM Tris, pH 7.5, 20% glycerol, 0.4 mg/ml salmon sperm DNA). Specificity was determined by adding a 100-fold excess of unlabeled competitor DNA to the reaction. For gel supershift analysis, nuclear proteins were incubated with antibodies against p65 protein, and gel-shift analysis was performed after adding labeled oligonucleotide.

ELISA. Aliquots were transferred to 96-well plates containing high-density immobilized oligonucleotide (5′-GGGACTTTCC-3′) (Trans-AM's ELISA; Active Motif, Carlsbad, CA). Anti-IgG HRP-conjugate and developing solution were added and read by spectrophotometry.

Western Blot. Cultures were lysed, and run on standard polyacrylamide gels, transferred to a nitrocellulose membrane, incubated in primary IgG antibody (1:1000), washed, incubated in alkaline phosphatase-linked secondary IgG antibody (1:2000), and imaged by chemiluminescence.

Reverse Transcriptase-PCR. Total RNA was prepared using TRIzol reagent (Invitrogen) and enriched for mRNA by an oligo(dT) spin-column kit (Oligotex; QIAGEN, Valencia, CA). mRNA was spectrophotometrically quantified and 40 ng of mRNA per reaction was used to synthesize first-strand cDNA (SuperScript RT-PCR System; Invitrogen). Semiquantitative PCR reaction aliquots were run on agarose and stained with ethidium bromide. PCR was performed for 28 and 30 cycles (1 min at 94°C, 1 min at 55°C, and 1 min at 72°C). Thirty cycles saturated the reaction. Duplicates of 28 cycle reactions were consistent with each other and were used for the results shown here. Primer sequences were: cyclophilin 5′-ATGGTCAACCCCACCGTGTT, cyclophilin 3′-CGTGTGAAGTCACCACCCT, p53left-TGAGCATCGAGCTC-CCTCTG, and p53right- CACAGGCCTCAGCTGGGATAGCACCTC.

Drugs. AMPA and *N*-methyl-D-aspartic acid were from Tocris Cookson Inc. (Ballwin, MO). Dizocilpine maleate, 1,2,3,4-tetrahydro-6-nitro-2,3-dioxo-benzo[*f*]quinoxaline-7-sulfonamide (NBQX), 1-napthyl-acetyl spermine trihydrochloride (NAS), *N*-benzyloxycarbonyl-Val-Ala-Asp-fluoromethyl ketone, cyclosporin A (CSA), 1-[bis(*p*-chlorophenyl)methyl]-3[2,4-dichloro-β-(2,4-dichlorobenzyloxy) phenethyl]-imidazolium chloride, 2,6-dimethyl-4-(2′-nitrophenyl)-3,5-pyridinecarboxylic acid dimethyl ester, and sodium 1-(*N*,*N*-diethylamino)diazen-1-ium-1,2-diolate (DEA/NO) were from Sigma-RBI (Natick, MA). 5,7-DHT, DTT, PMSF, and pyrrolidine dithiocarbamate (PDTC) were from Sigma-Aldrich (St. Louis, MO). DHR123 was from Molecular Probes (Eugene, OR). Boc-aspartyl-(OMe)-fluoromethyl ketone was from Enzyme Systems Products (Livermore, CA). Tacrolimus was from Fujisawa USA (Deerfield, IL). The HPNFκB oligonucleotide sequence (5′-AGTT-GAGGGGACTTTCCCAGGC-3′) and C-NFκB oligonucleotide sequence (5′-CTAATCTCCTCTAATCTCCCT-3′) were from the Nucleic Acid Chemistry Laboratory, Biotechnology Center, Washington University, (Saint Louis, MO).

Results

Morphological Characteristics of DNs Undergoing AMPA Toxicity. Treatment with AMPA for 24 h caused concentration-dependent death of DNs ($EC_{50} \approx 30$ μM), without significant change in MAP2-stained/TH-negative neurons (Fig. 1a). *N*-Methyl-D-aspartic acid (100–300 μM) failed to affect survival, and 3 μM dizocilpine failed to protect against AMPA toxicity (not shown). Surviving DNs showed neurite pruning, even after 10 μM AMPA (control, 1265 ± 109 μm; treated, 773 ± 81 μm). This AMPA concentration failed to elicit significant cell loss (Fig. 1, a and b). AMPA-induced pruning (shortening of neurites with loss of dendritic branching) (Fig. 1, c and d), was associated with loss of characteristic punctate synapsin staining along the neurites of DNs (Fig. 1, e and f). Ultrastructural analysis of DNs after 30 μM AMPA administration revealed nuclear invagination and irregular aggregation of chromatin consistent with excitotoxicity (Fig. 1, g-h) (Ishimaru et al., 1999).

AMPA Toxicity Requires Ca²⁺ Entry through Voltage-Dependent Channels. We reported previously that L-type Ca²⁺ channel (LTCC) blockers prevent AMPA-induced $[Ca^{2+}]_i$ elevations in the perikarya (but not dendrites) of DNs (de Erausquin et al., 1992). The LTCC blocker nimodipine (10 μM) reduced DN death (Fig. 2f) but only partially prevented pruning (in percentage of control length, nimodipine alone, 103.8 ± 10.6; +10 μM AMPA, 58.9 ± 9.0; +30 μM AMPA, 64.5 ± 7.5; +100 μM AMPA, 50.4 ± 6.2). Over 24 h, a small level of activation of Ca²⁺-permeable GluR$_{AMPA}$ could lead to DNs death. We compared the effects of two GluR$_{AMPA}$ antagonists, the nonselective NBQX (10 μM) and Joro spider toxin analog NAS (30 μM), which selectively blocks Ca²⁺-perme-

able receptors. NBQX reduced AMPA toxicity against DNs, whereas NAS was ineffective (Fig. 2a).

Time of Commitment to Die and Mitochodrial Permeability during AMPA Toxicity. Annexin V is a probe for translocation of PS to the outer leaflet of the cell membrane—an event that correlates with commitment to die (Vermes et al., 1995). We assessed PS translocation in DNs using Alexa 568-conjugated Annexin V (Fig. 2b) and TH immunostaining (Fig. 2,c). AMPA (30–100 μM) progressively increased annexin V binding in DNs between 3 and 16 h, before cell death was detected by propidium iodide staining (Fig. 2g). This staining was seldom observed in non-DNs (data not shown).

Because oxidative stress commonly follows Ca²⁺ overload (Hirsch et al., 1997), we studied ROS production in DNs using the fluorescent probe DHR123. Adding 100 μM AMPA for 10 min increased fluorescence in DNs (Fig. 3a, top) but not in nonDNs (Fig. 3b). Sham washes had no effect. Electron micrographs of DNs after 30 μM AMPA treatment for 3 h showed changes consistent with mitochondrial edema (Fig. 3, d and e). Cytochrome *c* (Cyt-c) release in DNs was measured
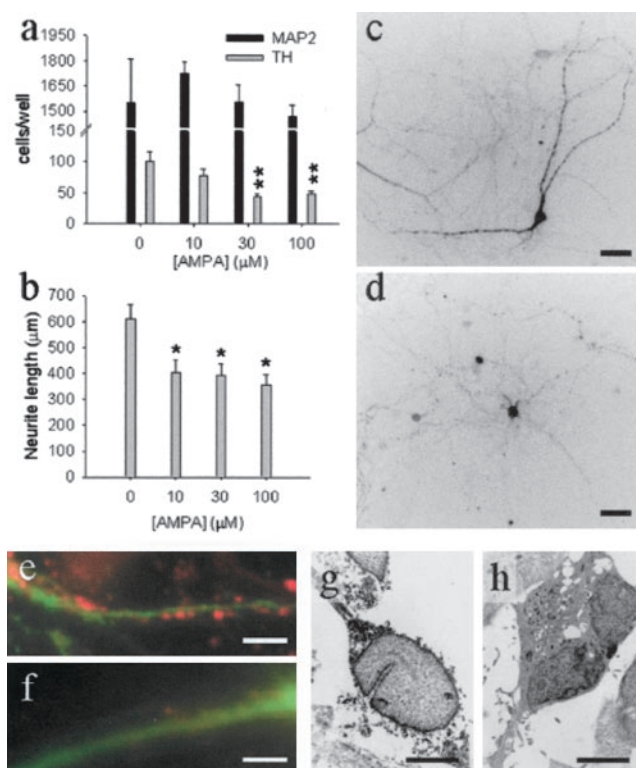
Fig. 1. Selective susceptibility of DNs to AMPA toxicity. Cultures were treated for 24 h with conditioned medium alone (control) or with 10, 30, or 100 μM AMPA. AMPA caused a loss of TH-stained neurons without significant change in MAP2-stained counts (a) (**, $p < 0.01$ compared with control). In TH-stained neurons, a concentration-dependent pruning is readily observed (b) (*, $p < 0.05$ compared with control). Examples of control (c) and 30 μM AMPA (d) are shown. About 50% of surviving treated DNs showed the changes demonstrated in d; the remainder showed varying degrees of pruning. Double staining with TH (green) and synapsin I (red) in control (e) and treated (f) cultures reveals loss of characteristic puncta in DNs after 30 μM AMPA treatment for 24 h; examples were chosen for their morphological integrity. Electron micrographs of DNs stained with TH/diaminobenzidine after 30 μM AMPA treatment for 3 h (h) or conditioned medium (g) taken at 3000× revealed nuclear invagination (nuclear perimeter in controls, 35.2 ± 1.2; AMPA, 41.8 ± 1.4; $p < 0.05$) and irregular clumps of chromatin condensation. Scale bars: c and d, 30 μm; e and f, 10 μm; g and h, 0.5 μm.

by monitoring the redistribution of immunostaining from punctated (mitochondrial) to diffuse (cytosolic). Treatment with 30 μM AMPA for 1 h induced redistribution of Cyt-c staining in TH stained neurons, consistent with release. Pixel distribution was normal after 3-h treatment (Fig. 3f), but at this time, total fluorescence was decreased, suggesting Cyt-c degradation. If mPT opening is required for cell death, preventing it should increase DNs survival. CSA (3 μM) protected DNs against AMPA toxicity (Fig. 3), whereas tacrolimus and calmidazolium were ineffective (Table 1). The inhibitor of the mitochondrial adenine nucleotide translocator, bongkrekic acid, also protected DNs (Fig. 3c). mPT opening may correlate with commitment to die, because addition of CSA 1 or 3 h after onset of 30 μM AMPA failed to provide an equal protection (Fig. 3g).

AMPA Toxicity Is Mediated by Transcriptional Activation of NFκB. Caspases mediate many forms of Cyt-c triggered cell death (Ravagnan et al., 2002). Two nonselective caspase inhibitors, *N*-benzyloxycarbonyl-Val-Ala-Asp-fluoromethyl ketone and Boc-aspartyl-(OMe)-fluoromethyl ketone, failed to prevent AMPA toxicity to DNs (Table 1). Immunostaining against activated caspase 3 was not detectable in DNs after AMPA treatment (not shown). Cell death triggered by oxidative stress in DNs is mediated by NFκB (Hunot et al., 1997). EMSA of NFκB DNA-binding proteins in nuclear extracts from cells exposed for 2 h to 30 μM AMPA revealed a band that shifted with anti-NFκBp65 antibody and was eliminated by excess unlabeled oligonucleotide but not by a random sequence oligonucleotide, C-NFκB (Fig. 4a). This band was absent in control extracts. When NFκB nuclear translocation was assessed by ELISA, 30 μM AMPA treatment for 2 h significantly increased

the specific signal; this increase was prevented by the decoy oligonucleotide HPNFκB but not by C-NFκB (Fig. 4b). NFκB is sequestered in the cytosol by the inhibitory protein, IκB; dissociation of IκB from NFκB is followed by degradation of IκB and nuclear translocation of NFκB (Thanos and Maniatis, 1995). IκB was markedly decreased in cell extracts after 30 μM AMPA for 1 h, with some recovery after 3 h (Fig. 4, c and d). Preventing NFκB activation with PDTC (Chung et al., 2000), dexamethasone, or HPNFκB, blocked AMPA toxicity (Fig. 4,e-g). C-NFκB had a marginally protective effect on cell survival, but did not prevent NFκB translocation. Its protective effect may be caused by mild nonspecific protein synthesis inhibition. We controlled for the antioxidant effect of PDTC with the spin trap reagents idebenone and PBN, as well as with the vitamin E analog trolox, all of which failed to protect DNs (Table 1). PDTC may protect neurons through inhibition of NO synthase (Hantraye et al., 1996), but in vitro NO release by itself may increase DNs viability (Mohanakumar et al., 1998). We tested the effect of the NOS inhibitors *N*-nitro-arginine and *N,N*-dimethyl-arginine and the NO donor DEA/NO on AMPA toxicity. NOS inhibitors marginally increased DNs survival, and DEA/NO increased AMPA toxicity (Table 1).

AMPA Toxicity Is Mediated by Activation of p53. RT-PCR products for p53, assessed by a semiquantitative assay normalized to the amount of cyclophilin, were elevated in each of four experiments after 30 μM AMPA treatment for 3 h. HPNFκB decreased the amount of p53 mRNA in control wells and prevented the increase induced by AMPA (Fig. 5, a and b). Treatment with 30 μM AMPA for 1 to 3 h increased phos-p53 protein in Western blots (Fig. 5, c and d), and immunohistochemistry revealed that this increase was restricted to DNs (Fig. 5, e and h); phos-p53 expression in DNs trends down after 3 h (Fig. 5i). The p53 inhibitor pifithrin-α, which reversibly blocks p53-dependent transcriptional activation and apoptosis (Komarov et al., 1999), protected DNs after 30 μM AMPA treatment for 24 h (Fig. 5j).

Discussion

Excitotoxicity has long been implicated in the pathophysiology of PD (Dunnett and Bjorklund, 1999) but no direct links between experimental and pathological data are available. For instance, hyperactivity of the glutamatergic subthalamic nucleus has been implicated in the generation of symptoms and in the progression of PD through excitotoxicity (Rodríguez et al., 1998). The data presented here suggest that the increase in NFκB nuclear translocation observed post-mortem in brains of PD patients may be caused by excitotoxicity.

AMPA toxicity to DNs caused cytosolic vacuolation, mitochondrial swelling, nuclear invagination, irregular chromatin clumping, and a loss of synaptic contacts. These changes are consistent with excitotoxicity but not with neuronal apoptosis (Ishimaru et al., 1999). Abnormal signaling seems also restricted to DNs, but we cannot categorically exclude indirect effects of the treatment on other neuronal phenotypes in the cultures. $GluR_{AMPA}$ stimulation results in a similar $[Ca^{2+}]_i$ increase in all neuronal phenotypes in our cultures, but only DNs fail to restore baseline $[Ca^{2+}]_i$ after AMPA removal (de Erausquin et al., 1994). LTCC antagonists prevent $[Ca^{2+}]_i$ influx to DNs during $GluR_{AMPA}$ stimulation, and blocking Ca^{2+} release from intracellular stores
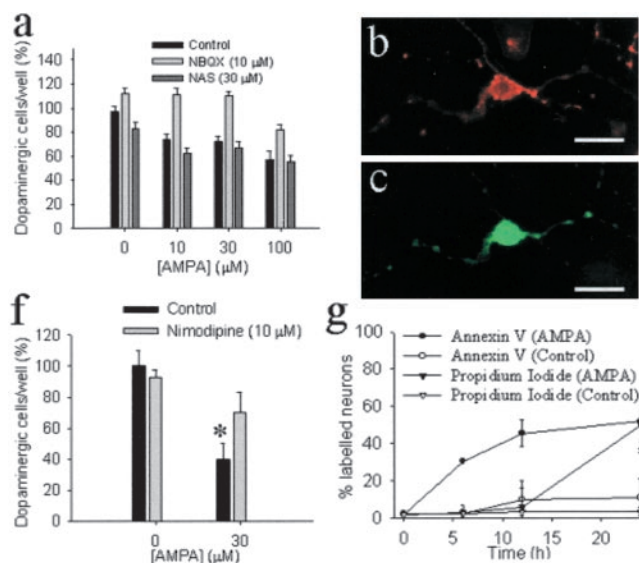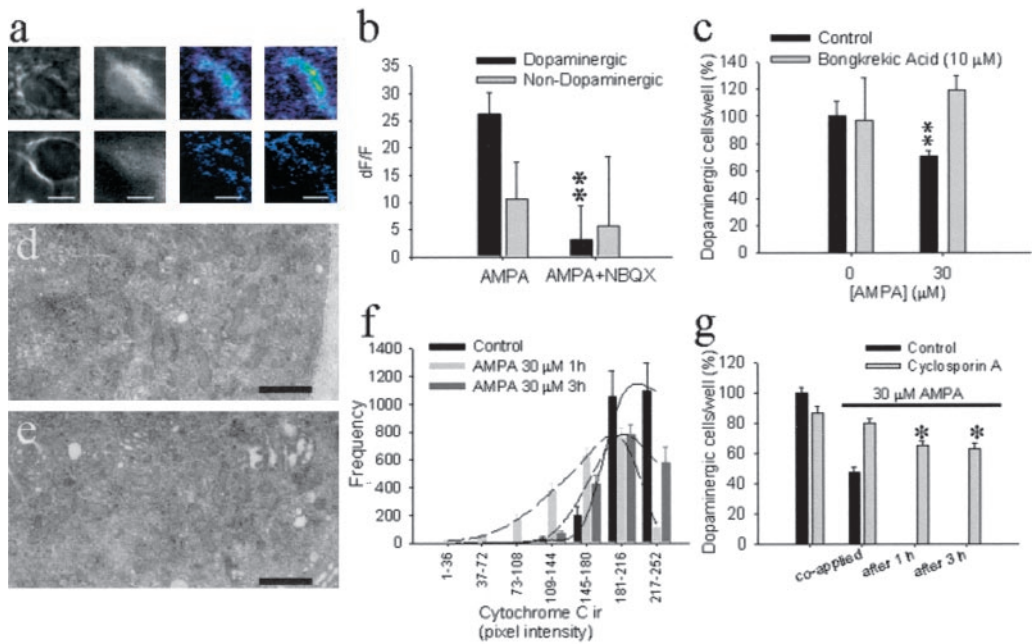
Fig. 2. AMPA toxicity to DNs requires opening of LTCC and is preceded by PS translocation. Cotreatment with 10 μM NBQX, but not 30 μM NAS, caused a left shift in the concentration-response curve of AMPA toxicity to DNs (a). Cotreatment with nimodipine (10 μM) significantly reduced the toxicity of 30 μM AMPA (f) (*, $p < 0.01$, mean ± S.E.M.). Double-staining of a DN after 100 μM AMPA treatment for 12 h with TH antibodies (b) and Annexin V-Alexa 568 (c). g shows time course of PS translocation as a percentage of the total count of DNs, and overlapping time course of propidium iodide uptake to monitor cell death. PS translocation increased significantly by 6 h ($p < 0.001$), whereas no significant changes in propidium iodide uptake were detected until 24 h. Spontaneous cell death in untreated cultures was less than 10% (mean ± S.E.M. Scale bar, 30 μm.

allows the return of $[Ca^{2+}]_i$ to baseline levels (de Erausquin et al., 1994). Now we show that LTCC opening is necessary for AMPA toxicity (Fig. 2f) However, LTCC antagonists had little effect on neurite pruning (data not shown), as expected because of the relative enrichment of N-type channels in neurites of DNs (de Erausquin et al., 1992). Our results also exclude the possibility that low levels of expression of Ca^{2+}-permeable $GluR_{AMPA}$ contribute significantly to toxicity, be-

cause the specific antagonist of Ca^{2+}-permeant $GluR_{AMPA}$, NAS, lacked protective effect.

The selectivity of AMPA toxicity may be because of a greater DNs susceptibility to oxidative stress. In fact, AMPA increased ROS in DNs but not in other neuronal phenotypes (Fig. 3, a and b). This increase in ROS was prevented by NBQX. Cell death can be triggered by Ca^{2+} overload leading to oxidative stress and mitochondrial release of Cyt-c (Ravagnan et al., 2002). We

Fig. 3. AMPA toxicity requires opening of a mPT. a shows, from left to right, phase contrast, 5,7-DHT, and DHR123 fluorescence images before (3rd) and after (4th) 20-min exposure to 100 μM AMPA alone (top row) or in combination with 10 μM NBQX (bottom row). An increase in DHR123 fluorescence was observed in DNs, which was not seen in other neurons (b) (mean ± S.E.M.; *, $p < 0.01$ compared with nondopaminergic neurons, $n =$ 20 neurons per group). NBQX prevented the change in fluorescence (a, bottom row, and b). d and e show electron micrographs of TH stained neurons taken at 11,500× in control conditions (d) or after 30 μM AMPA treatment for 3 h. Treatment resulted in swelling of mitochondria and endoplasmic reticulum (e). f shows a quantitative analysis of the distribution of Cyt-c immunostaining before or after 30 μM AMPA for 1 or 3 h. Culture dishes ($n =$ 3/condition) were fixed at the specified times and immunostained for TH and Cyt-c. Pictures of TH-stained neurons were taken blindly with respect to treatment, and the distribution of Cyt-c staining intensity in a region of interest excluding the nucleus was measured with an image analysis system. Punctate staining around the nuclear cup correlated with a distribution of intensities with a mode toward the brightest values. Cyt-c diffusion to the cytosol results in redistribution of pixel intensities along a normal distribution. The difference between these two distributions was statistically significant ($\chi^2 = 1979$, df = 20, $p < 0.001$). The mPT antagonists bongkrekic acid (10 μM, c; **, $p < 0.001$ compared with control) and CSA (3 μM, d) resulted in significant protection of DNs after treatment with 30 μM AMPA for 24 h. Addition of 3 μM CSA 1 or 3 h after onset of AMPA treatment resulted in reduced protection, with significant toxicity remaining ($p < 0.05$; *, $p < 0.01$ compared with control).

TABLE 1

Effect of neuroprotectants on DN survival after AMPA

Values represent mean of three experiments ± S.E.M. In each experiment, four to six wells per treatment were counted. MAP-2 counts did not vary significantly across categories. Cell counts were normalized between experiments to number of MAP-2 cells per well.

	Control	100 μM AMPA
No drug	111.0 ± 11.5	45.1 ± 9.4
Calmidazolium (3 μM)	104.0 ± 3.0	36.1 ± 2.0
Tacrolimus (0.1 μM)	96.9 ± 16.3	54.3 ± 14.3
C-NFκB (3.1 pmol/ml) (1:10,000)	121.3 ± 6.8	60.7 ± 6.8*
Cycloheximide (3 μg/ml)	89.2 ± 15.7	69.5 ± 8.0*
N-Benzyloxycarbonyl-Val-Ala-Asp-fluoromethyl ketone (100 μM)	88.8 ± 13.6	51.8 ± 13.6
Boc-aspartyl-(OMe)-fluoromethyl ketone (100 μM)	101.6 ± 6.0	41.6 ± 4.0
Idebenone (1 μM)	89.1 ± 15.1	50.3 ± 32.2
Trolox (3 μM)	159.9 ± 21.2	57.3 ± 33.2
Phenyl-t-butyl-nitrone (500 μM)	139 ± 10.1	42.5 ± 18.1
N,N-dimethyl-arginine (100 μM)	115 ± 7.1	63.2 ± 7.1
N,N-dimethyl-arginine (300 μM)	119 ± 8.1	80 ± 5.5*
DEA/NO (100 μM)	126.5 ± 6.7	17.5 ± 6.7#

* $P < 0.05$ compared with no drug.
** $P < 0.01$ compared with no drug.
# AMPA concentration was 30 μM in this experiments.

found evidence of mitochondrial swelling and Cyt-c release soon after exposure of DNs to toxic concentrations of AMPA. Consistent with these findings, the mPT antagonists CSA and bongkrekic acid blocked AMPA toxicity (Fig. 3c). The protective effect of CSA was significantly reduced if treatment began 1 h after onset of AMPA treatment, suggesting that mitochondrial changes occur at the time of commitment to die. This is in agreement with the time of commitment to die assessed by translocation of PS (Fig. 2g). CSA may protect neurons by preventing opening of mPT (Khaspekov et al., 1999; Matsumoto et al., 1999), but also by inhibiting calcineurin (Ankarcrona et al., 1996; Ruiz et al., 2000). Our results indicate that in DNs, AMPA toxicity does not require calmodulin-calcineurin activation, because calmidazolium and tacrolimus failed to afford protection (Table 1).

In DNs, Cyt-c release did not result in caspase 3 activation
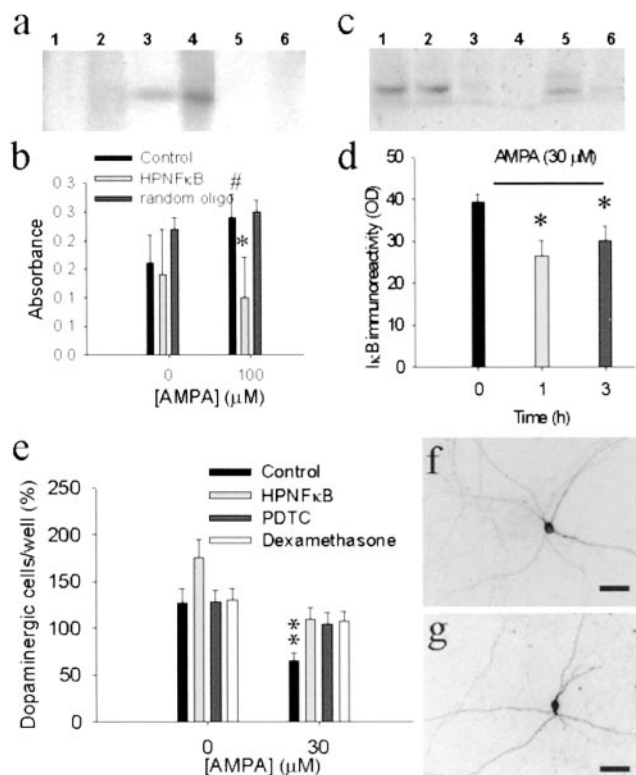
Fig. 4. NFκB nuclear translocation and transcriptional activity is required for AMPA toxicity. a shows an example of EMSA for NFκB p65 on nuclear extracts of mesencephalic cultures after 3-h treatment with conditioned medium alone (lanes 1–2) or with 30 μM AMPA (lanes 3–4). There is a strong induction of bound p65 after treatment. Lanes 5–6 were run in the presence of excess cold oligonucleotide containing the consensus binding sequence and confirmed the binding specificity. Two other experiments showed identical results. EMSA results were confirmed by a quantitative ELISA-based assay, and the effects of the oligonucleotides HPNFκB and C-NFκB were assessed (b). Absorbance data represent the average of three separate experiments (*, $P < 0.01$ versus 100 μM AMPA alone; #, $P < 0.05$ versus control). Expression of IκBα in cell extracts was assessed by Western blot (c and d). A 36-kDa band consistent with IkBα was detected in control lines (lanes 1 and 2) and was markedly decreased after 30 μM AMPA for 1 h (lanes 3 and 4) or 3 h (lanes 5 and 6). d shows average optical densities of three separate experiments (*, $P < 0.01$ versus 30 μM AMPA alone). e shows counts of DNs in cultures exposed to conditioned medium alone, with 30 μM AMPA by itself, or combined with HPNFκB (1:10,000 dilution of 3 pg/μl), 10 μM dexamethasone, or 300 μM PDTC. Data represent the average of three experiments (**, $P < 0.001$ versus control). Examples of TH stained neurons in control conditions (f) and after 30 μM AMPA + HPNFκB for 24 h (g) show protection of neurites.

(Table 1). This result prompts questions concerning the effector mechanism of cell death. Our data indicate that NFκB signaling plays a central role in AMPA toxicity to DNs. Two lines of evidence support this view. First, AMPA increases NFκB translocation and decreases expression of IκB, both at the time of commitment to die. Second, AMPA toxicity is prevented by three NFκB antagonists with different molecular mechanisms of action. PDTC has been shown to prevent or potentiate apoptosis, depending on cell type and culture conditions (Erl et al., 2000). We found that low concentrations of PDTC prevent AMPA toxicity (Fig. 4e). PDTC also has antioxidant properties, is a copper chelator, and inhibits NOS (Chen et al., 2000; Chung et al., 2000), but other antioxidants failed to protect DNs, and NOS inhibitors had limited effect, suggesting that PDTC protects DNs by NFκB inhibition. Even though NO release did not affect DNs viability by itself, it significantly potentiated the toxicity of AMPA, suggesting that ADP ribosylation may increase the
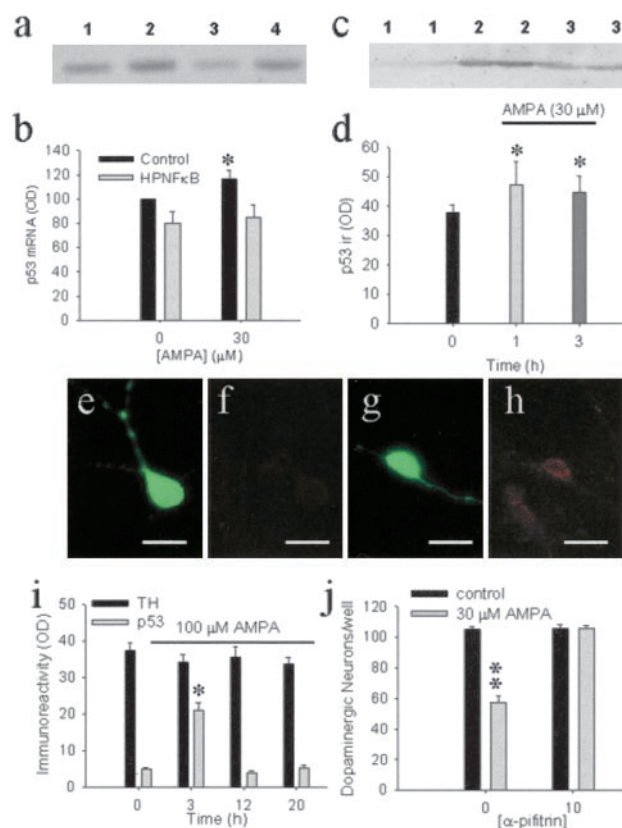
Fig. 5. Induction of p53 oncogene is required for AMPA toxicity. a, Northern blot of mesencephalic cultures extracts after 3-h exposure to conditioned medium (lane 1), 30 μM AMPA (lane 2), HPNFκB (1:10,000 dilution of 3 pg/μl, lane 3), and AMPA + HPNFκB (lane 4). Optical density averages of four experiments are shown in b (*, $p < 0.001$ versus control by analysis of variance on ranks). Western blots of phos-p53 are shown in c and d. A 53-kDa band consistent with p53 was detected in control lanes (1–2), which was increased after 30 μM AMPA for 1 h (lanes 3 and 4) or 3 h (lanes 5 and 6). d shows average optical densities of three separate experiments (*, $P < 0.01$ versus 30 μM AMPA alone). Cellular localization of phos-p53 was assessed by immonocytochemistry (e and h). phos-p53 was not detected in nondopaminergic neurons. TH-stained neurons exposed to conditioned medium (e) did not have detectable phos-p53 immunoreactivity (f) but were stained after 100 μM AMPA for 3 h (g and h). Quantitative image analysis of TH positive neurons demonstrated no change in TH expression but a transient increase in phos-p53 at 3 h (i). (*, $p < 0.01$). DNs counts in cultures exposed to conditioned medium alone, with 30 μM AMPA by itself, or combined with 10 μM pifithrin-α, showed complete protection by the antagonist (j) (**, $P < 0.001$ versus control).

susceptibility of DNs. Indeed, the ADP ribosylation antagonist benzamide resulted in a degree of protection similar to that of NOS inhibitors (data not shown).

Increased NFκB nuclear translocation in PD brains postmortem has been interpreted as evidence of activation of the TNFα pathway (Hunot et al., 1997). Our data suggest that sustained GluR$_{AMPA}$ activation could induce the same result. This finding is potentially very important, if confirmed in vivo, because excitotoxicity may be sustained chronically in PD by subthalamic nucleus hyperactivity. Neuronal NFκB is activated by GluR$_{AMPA}$ stimulation (Kaltschmidt et al., 1995), causing cell death in some—including mesencephalic—neuronal phenotypes (Hunot et al., 1997; Schneider et al., 1999; Cassarino et al., 2000) but protecting others against apoptosis (Mattson et al., 2000). In neurons, NFκB transcriptional activation causes cell death mediated through p53 (Ryan et al., 2000). Our data suggest that in DNs, transcriptional activation of NFkB causes transcription of p53 mRNA, because HPNFκB prevented the increase in p53 mRNA induced by AMPA (Fig. 5). Also, increased phos-p53 expression was restricted to DNs (Fig. 5, c, g, and h) and was necessary for toxicity, because the p53 inhibitor pifithrin-α completely prevented DN death. The mechanism of action of pifithrin-α has not been completely elucidated, but it seems to act downstream of p53 and may modulate nuclear import or export of p53 or decrease the stability of nuclear p53 (Komarov et al., 1999).

In summary, we have shown that embryonic DNs are selectively susceptible to overactivation of GluR$_{AMPA}$, resulting in neuronal death mediated through transcriptional activation of NFκB. AMPA toxicity, if our findings are confirmed in vivo, may be a good candidate target for neuroprotection of DNs in patients with PD.

Acknowledgments

References

Anglade P, Vyas S, Javoy-Agid F, Herrero MT, Michel PP, Marquez J, Mouatt-Prigent A, Ruberg M, Hirsch EC, and Agid Y (1997) Apoptosis and autophagy in nigral neurons of patients with Parkinson's disease. *Histol Histopathol* **12**:25–31.

Ankarcrona M, Dypbukt JM, Orrenius S, and Nicotera P (1996) Calcineurin and mitochondrial function in glutamate-induced neuronal cell death. *FEBS Lett* **394**:321–324.

Bywood PT and Johnson SM (2000) Differential vulnerabilities of substantia nigra catecholamine neurons to excitatory amino acid-induced degeneration in rat midbrain slices. *Exp Neurol* **162**:180–188.

Cassarino DS, Halvorsen EM, Swerdlow RH, Abramova NN, Parker WD, Sturgill TW, and Bennett JP (2000) Interaction among mitochondria, mitogen-activated protein kinases and nuclear factor-kappaB in cellular models of Parkinson's disease. *J Neurochem* **74**:1384–1392.

Chen SH, Liu SH, Liang YC, Lin JK, and Lin-Shiau SY (2000) Death signaling pathway induced by pyrrolidine dithiocarbamate-Cu^{2+} complex in the cultured rat cortical astrocytes. *Glia* **31**:249–261.

Chung KC, Park JH, Kim CH, Lee HW, Sato N, Uchiyama Y, and Ahn YS (2000) Novel biphasic effect of pyrrolidine dithiocarbamate on neuronal cell viability is mediated by the differential regulation of intracellular zinc and copper ion levels, NF-kappaB and MAP kinases. *J Neurosci Res* **59**:117–125.

Damier P, Hirsch EC, Agid Y, and Graybiel AM (1999) The substantia nigra of the human brain. II. Patterns of loss of dopamine-containing neurons in Parkinson's disease. *Brain* **122**:1437–1448.

de Erausquin GA, Brooker G, and Hanbauer I (1992) K$^+$-evoked dopamine release depends on a cytosolic Ca^{2+} pool regulated by N-type Ca^{2+} channels. *Neurosci Lett* **145**:121–125.

de Erausquin GA, Brooker G, Costa E, and Hanbauer I (1994) Persistent AMPA receptor stimulation alters [Ca^{2+}]$_i$ homeostasis in cultures of embryonic dopaminergic neurons. *Brain Res Mol Brain Res* **21**:303–311.

Dugan LL, Sensi SL, Canzoniero LM, Handran SD, Rothman SM, Lin TS, Goldberg MP, and Choi DW (1995) Mitochondrial production of reactive oxygen species in

cortical neurons following exposure to N-methyl-D-aspartate. *J Neuroscience* **15**:6377–6388.

Dunnett SB and Bjorklund A (1999) Prospects for new restorative and neuroprotective treatments in Parkinson's disease. *Nature (Lond)* **399**(Suppl.):A32–A39.

Erl W, Weber C, and Hansson GK (2000) Pyrrolidine dithiocarbamate-induced apoptosis depends on cell type, density and the presence of Cu^{2+} and Zn^{2+}. *Am J Physiol* **278**:C1116–C1125.

German DC, Manaye KF, Sonsalla PK, and Brooks BA (1992) Midbrain dopaminergic cell loss in Parkinson's disease and MPTP-induced parkinsonism: sparing of calbindin-D28k-containing cells. *Ann NY Acad Sci* **648**:42–62.

Hantraye P, Brouillet E, Ferrante R, Palfi S, Dolan R, Matthews RT, and Beal MF (1996) Inhibition of neuronal nitric oxide synthase prevents MPTP-induced parkinsonism in baboons. *Nat Med* **2**:1017–1021.

Hartmann A, Mouatt-Prigent A, Faucheux BA, Agid Y, and Hirsch EC (2002) FADD: a link between TNF family receptors and caspases in Parkinson's disease. *Neurology* **58**:308–310.

Hirsch EC, Brandel JP, Galle P, Javoy-Agid F, and Agid Y (1991) Iron and aluminum increase in the substantia nigra of patients with Parkinson's disease: an X-ray microanalysis. *J Neurochem* **56**:446–451.

Hirsch EC, Faucheux B, Damier P, Mouatt-Prigent A, and Agid Y (1997) Neuronal vulnerability in Parkinson's disease. *J Neural Transm Suppl* **50**:79–88.

Hunot S, Brugg B, Ricard D, Michel PP, Muriel MP, Ruberg M, Faucheux BA, Agid Y, and Hirsch EC (1997) Nuclear translocation of NF-kappaB is increased in dopaminergic neurons of patients with Parkinson disease. *Proc Natl Acad Sci USA* **94**, 7531–7536.

Isaacs KR, de Erausquin GA, Strauss KI, Jacobowitz DM, and Hanbauer I (1996) Differential effects of excitatory amino acids on mesencephalic neurons expressing either calretinin or tyrosine hydroxylase in primary cultures. *Brain Res Mol Brain Res* **36**:114–126.

Ishimaru MJ, Ikonomidou C, Tenkova TI, Der TC, Dikranian K, Sesma MA, and Olney JW (1999) Distinguishing excitotoxic from apoptotic neurodegeneration in the developing rat brain. *J Comp Neurol* **408**:461–476.

Jellinger KA, Kienzl E, Rumpelmaier G, Paulus W, Riederer P, Stachelberger H, Youdim MB, and Ben-Shachar D (1993) Iron and ferritin in substantia nigra in Parkinson's disease. *Adv Neurol* **60**:267–272.

Jellinger KA (2001) Cell death mechanisms in neurodegeneration. *J Cell Mol Med* **5**:1–17.

Jenner P (1998) Oxidative mechanisms in nigral cell death in Parkinson's disease. *Mov Disord* **13**(Suppl)**1**:24–34.

Kaltschmidt C, Kaltschmidt B, and Baeuerle PA (1995) Stimulation of ionotropic glutamate receptors activates transcription factor NF-kappa B in primary neurons. *Proc Natl Acad Sci USA* **92**:9618–9622.

Khaspekov L, Friberg H, Halestrap A, Viktorov I, and Wieloch T (1999) Cyclosporin A and its nonimmunosuppressive analogue N-Me-Val-4-cyclosporin A mitigate glucose/oxygen deprivation-induced damage to rat cultured hippocampal neurons. *Eur J Neurosci* **11**:3194–3198.

Komarov PG, Komarova EA, Kondratov RV, Christov-Tselkov K, Coon JS, Chernov MV, and Gudkov AV (1999) A chemical inhibitor of p53 that protects mice from the side effects of cancer therapy. *Science (Wash DC)* **285**, 1733–1737.

Matsumoto S, Friberg H, Ferrand-Drake M, and Wieloch T (1999) Blockade of the mitochondrial permeability transition pore diminishes infarct size in the rat after transient middle cerebral artery occlusion. *J Cereb Blood Flow Metab* **19**:736–741.

Mattson MP, Culmsee C, Yu Z, and Camandola S (2000) Roles of nuclear factor kappaB in neuronal survival and plasticity. *J Neurochem* **74**:443–456.

McNaught KS and Jenner P (2001) Proteasomal function is impaired in substantia nigra in Parkinson's disease. *Neurosci Lett* **297**:191–194.

Mochizuki H, Goto K, Mori H, and Mizuno Y (1996) Histochemical detection of apoptosis in Parkinson's disease. *J Neurol Sci* **137**:120–123.

Mohanakumar KP, Hanbauer I, and Chiueh CC (1998) Neuroprotection by nitric oxide against hydroxyl radical-induced nigral neurotoxicity. *J Chem Neuroanat* **14**:195–205.

Ravagnan L, Roumier T, and Kroemer G (2002) Mitochondria, the killer organelles and their weapons. *J Cell Physiol* **192**:131–137.

Rodríguez MC, Obeso JA, and Olanow CW (1998) Subthalamic nucleus-mediated excitotoxicity in Parkinson's disease: a target for neuroprotection. *Ann Neurol* **44**(3 Suppl 1)**:**S175–S188.

Ruiz F, Alvarez G, Ramos M, Hernandez M, Bogonez E, and Satrustegui J (2000) Cyclosporin A targets involved in protection against glutamate excitotoxicity. *Eur J Pharmacol* **404**:29–39.

Ryan KM, Ernst MK, Rice NR, and Vousden KH (2000) Role of NF-kappaB in p53-mediated programmed cell death. *Nature (Lond)* **404**:892–897.

Schneider A, Martin-Villalba A, Weih F, Vogel J, Wirth T, and Schwaninger M (1999) NF-kappaB is activated and promotes cell death in focal cerebral ischemia. *Nat Med* **5**:554–559.

Silva NL, Mariani AP, Harrison NL, and Barker JL (1988) 5, 7-Dihydroxytryptamine identifies living dopaminergic neurons in mesencephalic cultures. *Proc Natl Acad Sci USA* **85**:7346–7350.

Thanos D and Maniatis T (1995) Virus induction of human IFN beta gene expression requires the assembly of an enhanceosome. *Cell* **80**:529–532.

Vermes I, Haanen C, and Steffens-Nakken H (1995) A novel assay for apoptosis. Flow cytometric detection of phosphatidylserine expression on early apoptotic cells using fluorescein labelled Annexin V. *J Immunol Methods* **184**:39–51.

Address correspondence to: Gabriel A. de Erausquin, MD, PhD, Departments of Psychiatry and Neurology, CSNSI, Washington University School of Medicine, 660 S. Euclid Ave, Campus Box 8134, St. Louis, MO 63110. E-mail: erausquing@neuro.wustl.edu